

# Synthesis of Polystyrene-Grafted Polyorganosiloxane Microgels and Their Compatibility with Linear Polystyrene Chains

Gudrun Lindenblatt,<sup>†</sup> Wolfgang Schärtl,<sup>\*,†</sup> Tadeusz Pakula,<sup>‡</sup> and Manfred Schmidt<sup>†</sup>

*Institut für Physikalische Chemie, Universität Mainz, Welterweg 11, 55099 Mainz, Germany, and Max-Planck Institut für Polymerforschung, Ackermannweg 10, 55021 Mainz, Germany*

*Received July 28, 2000; Revised Manuscript Received October 3, 2000*

**ABSTRACT:** We describe the preparation of hairy nanospheres by grafting of polystyrene macromonomer chains onto polyorganosiloxane microgels. Our strategy was to obtain special surface-modified colloidal particles, which can be blended with linear polymer chains without depletion demixing found for standard colloid–polymer mixtures. For this purpose, the molecular weight of the polymer hairs and of the linear chains has been varied between 4000 and 19 000 g/mol. In all cases, the number of hairs per single particle with core radius about 10 nm exceeded 150. Studying the internal structure of mixtures of these hairy spheres with linear polymer chains by transmission electron microscopy and small-angle X-ray scattering, we identified homogeneous systems, i.e., suppression of depletion demixing, in case the molecular weight of the polymer hairs on the particle surface is at least as large as the molecular weight of the single polymer chains. This result is interpreted in terms of a new depletion model, taking into account the surface roughness of colloidal spheres with a surface of polymer hairs, and the probability of single polymer chains to partially penetrate into this hairy particle surface.

## Introduction

Colloidal nanoparticles as fillers for thermoplastic or elastic polymers are very useful to improve the mechanical properties of the materials. A popular example is carbon black blended into polyisoprene to enhance the mechanical stability of tire rubber.

For a maximum effect, the colloidal additives should be homogeneously dispersed within the polymer matrix. However, standard colloidal particles usually are entropically incompatible with linear polymer chains and show a macroscopic phase separation.<sup>1–3</sup> This so-called depletion demixing has first been described theoretically by Asakura and Oosawa.<sup>1</sup> The existence of depletion attraction due to entropic effects has been verified experimentally by Bechinger et al.<sup>4</sup> The principle of depletion is sketched in Figure 1:

For a given system of large colloidal spheres and smaller linear polymer chains, there is an entropic balance between the structural entropy of the spherical particles and the free volume entropy of the linear chains. The rigid surface of the colloids does not allow for penetration of the linear chains and therefore creates an excluded volume with shell thickness comparable to the radius of the polymer coil (see Figure 1, dotted line). If two colloidal particles aggregate, their excluded-volume zones overlap, causing a decrease in total excluded volume and a corresponding increase in free volume accessible for the polymer chains. In case the gain in entropy due to this increase in free volume is larger than the entropy loss due to aggregation of the spherical colloids, the entropic balance favors depletion demixing. Here, it should be noted that the same principle also holds for a mixture of large and small spherical colloids with rigid nonpenetrable surfaces.

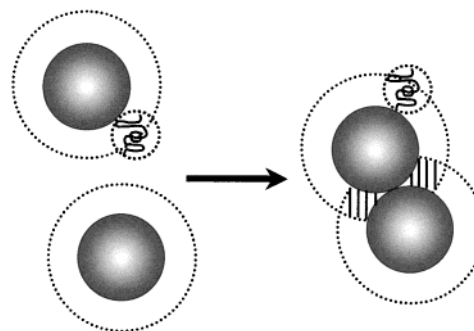


**Figure 1.** Sketch of depletion demixing of spherical colloidal particles (with smooth nonpenetrable particle surface) and linear polymer chains. See text for discussion.

There are few strategies to overcome this depletion demixing, i.e., to prepare homogeneous colloid–polymer blends, found in the literature. An important possibility used by Mark et al.<sup>5,6</sup> is to dissolve the colloidal particles in a monomer solution which next is polymerized, thereby kinetically trapping the colloids within a homogeneous particle distribution. Note, however, that such systems are not in thermodynamic equilibrium and therefore may change their structure with temperature.

In this article, we present a method to prepare thermodynamically stable homogeneous mixtures of colloidal particles and linear polymer chains. Our strategy is deduced from homogeneous mixtures of spherical copolymer micelles and linear polymer chains chemically identical to the micellar corona, a system well-known in the literature. Previously, we have investigated frozen micelles with a glassy polystyrene (PS) core and a polyisoprene (PI) corona, embedded in a matrix of linear PI.<sup>7–10</sup> For these systems with molecular weight of the corona PI block equal to or larger than the molecular weight of the matrix homopolymer, the distribution of micelles studied by small-angle X-ray scattering (SAXS) has been found to be homogeneous. Therefore, depletion demixing of colloids

<sup>†</sup> Universität Mainz.

<sup>‡</sup> Max-Planck Institut für Polymerforschung.

\* To whom correspondence should be addressed. E-mail: schuertl@mail.uni-mainz.de.

and polymers seems to be suppressed if the colloidal particles are coated with a polymeric surface. In this respect, copolymer micelles seem to be an ideal system to prepare homogeneous colloid–polymer blends. However, these particles are only formed by self-organization in situ and are not formed at all if the copolymer concentration is lower than the critical micellar concentration, which in the case of our PS–PI system according to recent small-angle neutron scattering (SANS) measurements is the order of 1 wt %. Therefore, to prepare colloid–polymer systems with arbitrary composition, colloidal particles with polymeric surface and with a fixed structure, which can be isolated as single supramolecules, are much better suited than copolymer micelles. Another disadvantage of copolymer micelles is the impossibility to vary the number of corona hairs per particle, at a given corona block molecular weight, without changing the size of the core of the micelles.

For these reasons, we have developed a new system of colloidal particles with polymeric surfaces, which are prepared by grafting of polymeric chains onto a pre-formed colloidal core. These supramolecules can be isolated, and the grafting density for a given colloidal core can be varied in a simple way. Our article is organized as follows: first, we describe the synthesis of polyorganosiloxane microgels grafted with linear polymer chains. Next, the particle characteristics such as particle size or number of hairs per particle will be presented. Last but not least, we have investigated the compatibility of our new colloidal particles with linear polymer chains. In this section, analogous to Figure 1, a modified depletion model will be sketched taking into account a finite interpenetrability of the surface of the colloidal particles.

## Experimental Section

**Preparation of Polystyrene-Grafted Polyorganosiloxane Microgels.** Polyorganosiloxane microgels are highly cross-linked spherical particles formed by polycondensation of trimethoxymethylsilane ( $\text{CH}_3\text{Si}(\text{OCH}_3)_3$ ) in aqueous emulsion.<sup>11,12</sup> The specialty of this system is the so-called end-capping reaction, i.e., a saturation of the reactive  $\text{Si}-\text{OCH}_3$  groups at the particle surface in emulsion with monosilane ( $(\text{CH}_3)_3\text{SiOCH}_3$ ). Thereby, the particle surface not only is made hydrophobic but also stabilized versus interparticle condensation. These nanoparticles can be isolated and redispersed in nonpolar organic solvents up to very high particle concentrations (>50 wt %). Another important feature of these microgels is that functional silanes can be used as comonomers, thereby providing a synthetic route to dye-labeled colloids<sup>13,14</sup> or particles doped with tiny metal clusters,<sup>15,16</sup> both of which have successfully been used in optical tracer diffusion measurements. The details of the synthesis of such microgels have been described previously. To prepare polyorganosiloxane microgels with polymeric coating, we have chosen a hydrosilylation reaction for grafting onto polystyrene chains on the microgel surface. Preliminary experimental results of this approach already have been published.<sup>17</sup> The reaction scheme is given in Figure 2.

Hydrosilylation comprises the chemical coupling between a SiH functionality and a vinylic double bond in the presence of a platinum catalyst.<sup>18</sup> Therefore, we need two components for preparation of PS-grafted microgels: (i) a microgel whose surface is functionalized with SiH groups; (ii) PS chains which are end-functionalized with a  $\text{C}=\text{C}$  bond, i.e., so-called PS macromers.

**(i) Preparation of a Surface-Functionalized Polyorganosiloxane Microgel.** First, a highly cross-linked core is formed by polycondensation of trimethoxymethylsilane in

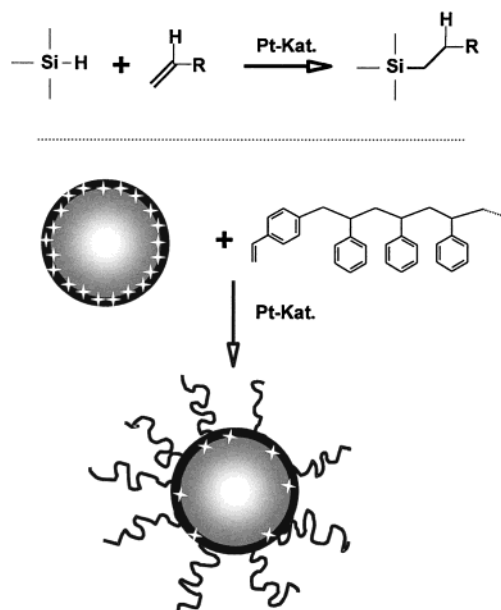


**Figure 2.** Sketch of the grafting-onto reaction of end-functionalized polystyrene chains onto polyorganosiloxane microgels by hydrosilylation. White stars =  $\text{Si}-\text{H}$  functional groups on the surface of the microgel.

aqueous emulsion, using dodecylbenzenesulfonic acid as both surfactant and catalyst. Second, the particle surface is functionalized with anchor groups suitable for the grafting-onto reaction according to a hydrosilylation mechanism. For this purpose, dihydridotetramethyldisiloxane ( $\text{H}(\text{CH}_3)_2\text{Si}-\text{O}-\text{Si}(\text{CH}_3)_2\text{H}$ ) is used as a functional end-capping agent, i.e., to saturate the  $\text{Si}-\text{OCH}_3$  groups at the particle surface with  $-\text{Si}(\text{CH}_3)_2\text{H}$  groups. These particles are isolated and redispersed in toluene. Details of this synthesis are given in the Appendix.

**(ii) Preparation of End-Functionalized PS Chains.** PS macromers are prepared by living anionic polymerization of styrene, using *sec*-butyllithium as an initiator and either benzene at  $T = 40^\circ\text{C}$  (molecular weight  $M_w < 10\,000$  g/mol) or tetrahydrofuran (THF) at  $T = -90^\circ\text{C}$  ( $M_w > 10\,000$  g/mol) as solvent. For termination, the solution containing the “living anionic” polymer chains is added dropwise into a solution containing an excess of *p*-bromomethylstyrene in THF. By Maldi-TOF mass spectrometry, we have confirmed the low polydispersity of our functional PS chains ( $M_w/M_n < 1.04$ ) as well as the high degree of functionalization which is nearly 100%.

Finally, it should be mentioned that, for preparation of the PS chains used as a polymer matrix in the colloid–polymer mixtures, the “living anionic” chains whose preparation has been described above simply have been terminated with methanol.

**(iii) Grafting of PS Macromers onto SiH-Functionalized Microgels.** For the grafting reaction, functionalized microgels (i) and PS macromers (ii) are dissolved in toluene, and a special platinum catalyst (Karstedt catalyst in toluene (3 wt %), Wacker Corp.) is added. The mixture is stirred at room temperature for several hours. The progress of the reaction is studied by gel permeation chromatography (GPC) with refractive index detection (PSS styragel columns, Waters differential refractometer detector). A typical GPC elugram, taken from a solution of 3 g of microgels and 2 g of PS macromers of molecular weight  $M_w = 9900$  g/mol in 50 mL of toluene before addition of the Pt catalyst and after a reaction time of 2 and 48 h, respectively, is shown in Figure 3.

The small peaks indicated by the arrows correspond to the microgel without and with grafted PS, whereas the large peak corresponds to the single PS macromer chains. With increasing reaction time, the macromer peak is decreasing, whereas the microgel peak is shifted toward smaller elution time, i.e., higher molecular weight. Also, the latter changes from nega-

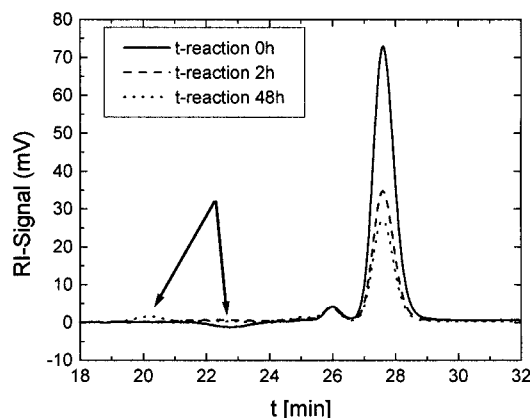


**Figure 3.** GPC signal (detection of refractive index) of a mixture of SiH-functionalized microgels and polystyrene macromonomers ( $M_w = 10\,000$  g/mol) before the reaction has been started (solid line) and 2 h (dashed line) and 48 h (dotted line) after the catalyst has been added.

tive to positive, corresponding to a change of the refractive index increment ( $dn/dc$ ), which is negative for microgels without PS coating in toluene ( $(dn/dc) = -0.042$  mL/g). Since the refractive index increment of PS in toluene is positive ( $(dn/dc) = +0.106$  mL/g), microgels grafted with a certain amount of PS chains also may show an average positive ( $dn/dc$ ) in toluene. Comparison of the refractive index increment of PS-grafted microgels with that of the microgel cores and the PS macromers allows to quantify the number of hairs per particle, as will be shown later.

If no further progress of the grafting reaction is detected in the GPC elugrams, nongrafted single PS macromer chains are removed by ultrafiltration of the toluene solution at a pressure 4–5 bar with a stirred ultrafiltration cell (Millipore XFUF 07601), using membranes with pore sizes suitable to retain the colloidal particles (Millipore PLTK076 NMWL30000 and NMWL100000).

**Particle Characterization.** The molecular weight  $M_w$  of the colloidal particles (before grafting) is determined by static light scattering, using a home-built setup for simultaneous multiangle light scattering equipped with a Stabilite 2060-45 Ar laser operating at a wavelength of 514 nm. The refractive index increments needed to determine  $M_w$  and used to calculate the number of hairs per particle have been measured with a home-built Michelson interferometer. All these measurements have been performed on toluene solutions.

The molecular weight of the PS macromers has been determined both by MALDI-TOF (Micromass TOFSpec-E spectrometer) and by GPC (Abimed autosampler 254, Rheos 400-HPLC-pump, set of 3 PSS styragel columns (pore size  $10^5$ ,  $10^4$ , and  $10^3$  Å), Waters differential refractometer detector, and Waters 486-UV/vis detector), using calibration with PS standards from PSS corporation for the later.

The hydrodynamic radii  $R_H$  of the colloidal particles without and with polymer grafted onto the surface have been determined by dynamic light scattering on toluene solutions, using a commercial setup from ALV (goniometer SP125, spectra physics 2060-4S Ar laser (514 nm) and ALV-5000 digital correlator).

Colloidal particles have been visualized by transmission electron microscopy, using an EM 420 ST (120 kV) from Philips. For these studies, samples have been prepared by solution casting of toluene solutions.

**Determination of the Number of PS Hairs per Particle.** The number of PS hairs per microgel has been determined in three different ways:

(1) If the molecular weight of the microgels before grafting and that of the PS macromers are known, the number of hairs per particle after grafting can be determined from the RI signal of the GPC elution curves shown in Figure 3. The decrease in peak area of the single macromer peak corresponds to the amount of macromer grafted onto the particle surface.

(2) The refractive index increment of the PS-grafted particles depends on the refractive index increments of nongrafted microgel (M) and PS macromer (PS) according to

$$\frac{dn}{dc} = x_M \left( \frac{dn}{dc} \right)_M + x_{PS} \left( \frac{dn}{dc} \right)_{PS} \quad (1)$$

with  $x_M$  and  $x_{PS}$  the molecular weight fraction of microgel core and PS macromer hairs. Since  $x_M + x_{PS} = 1$ , according to eq 1 the average number of hairs per particle can be calculated if all refractive index increments and the molecular weight of microgel and PS macromer are known.

(3) UV absorption spectroscopy also can be used to determine the amount of grafted PS per microgel. Whereas PS shows strong light absorption between 250 and 300 nm, the microgels do not absorb light in this wavelength regime. Using standard solutions of pure PS in THF for calibration, the PS content of a THF solution of PS-grafted microgels could be quantified.

**Preparation of Colloid–Polymer Mixtures.** Colloid–polymer mixtures have been prepared by solution casting from THF solution. The appropriate amount of PS chains and of colloidal particles are dissolved in THF, total solid content about 10 wt %. The solvent is slowly evaporated at room temperature and normal pressure. To remove all solvent and for equilibration, the as-cast films are vacuum-annealed for several days at a temperature 20 °C above the glass transition of the PS matrix chains (typically at 120 °C).

**Characterization of Colloid–Polymer Mixtures.** The structure of the colloid–polymer mixtures has been characterized by transmission electron microscopy and by small angle X-ray scattering:

(1) The blend structure, that is, the distribution of microgel cores within the polystyrene matrix, has been visualized by transmission electron microscopy, using an EM 420 ST (120 kV) from Philips. For these studies, samples have been prepared by solution casting of toluene solutions as described above. Next, thin slices of thickness a few micrometers have been cut from the as-cast and annealed films using a microtome.

(2) Small-angle X-ray scattering (SAXS) has been used to investigate the structure of the mixtures in a more quantitative way. Our setup consisted of an 18 kW rotating anode (Rigaku) with pinhole collimation as a source and a two-dimensional detector (Siemens) with  $512 \times 512$  pixels. A double graphite monochromator for the Cu K $\alpha$  radiation ( $\lambda = 0.154$  nm) was used. The beam diameter was about 1 mm, and the evacuated sample-to-detector path was 1.2 m. The 2D scattering patterns have been integrated in order to get the scattered intensity distribution as a function of the scattering vector  $s (= 2 \sin(\theta/2)/\lambda)$ , with  $\theta$  the scattering angle.

## Results and Discussion

**Characterization of PS-Grafted Microgels.** Transmission electron microscopy has been used to visualize the new particles. Samples have been prepared by solution casting from toluene solutions. During evaporation of the solvent, cohesion leads to the formation of 2D close-packed clusters of the colloidal particles. Interestingly, due to the difference in electron density, there is a large contrast between the polyorganosiloxane cores of the grafted particles and their PS shell. Therefore, in Figure 4 only the polyorganosiloxane cores are visible, whereas the grafted PS layer remains invisible in the TEM pictures. As a consequence, grafted particles presented in Figure 4 show a clear separation of their polyorganosiloxane cores, even though all particles are in close contact with each other (Figure 4b,c). Obviously, the optical separation between polyorganosiloxane cores of grafted particles increases with the molecular weight of the PS hairs, i.e., with the thickness of the grafted PS layer. On the other hand, polyorganosiloxane par-



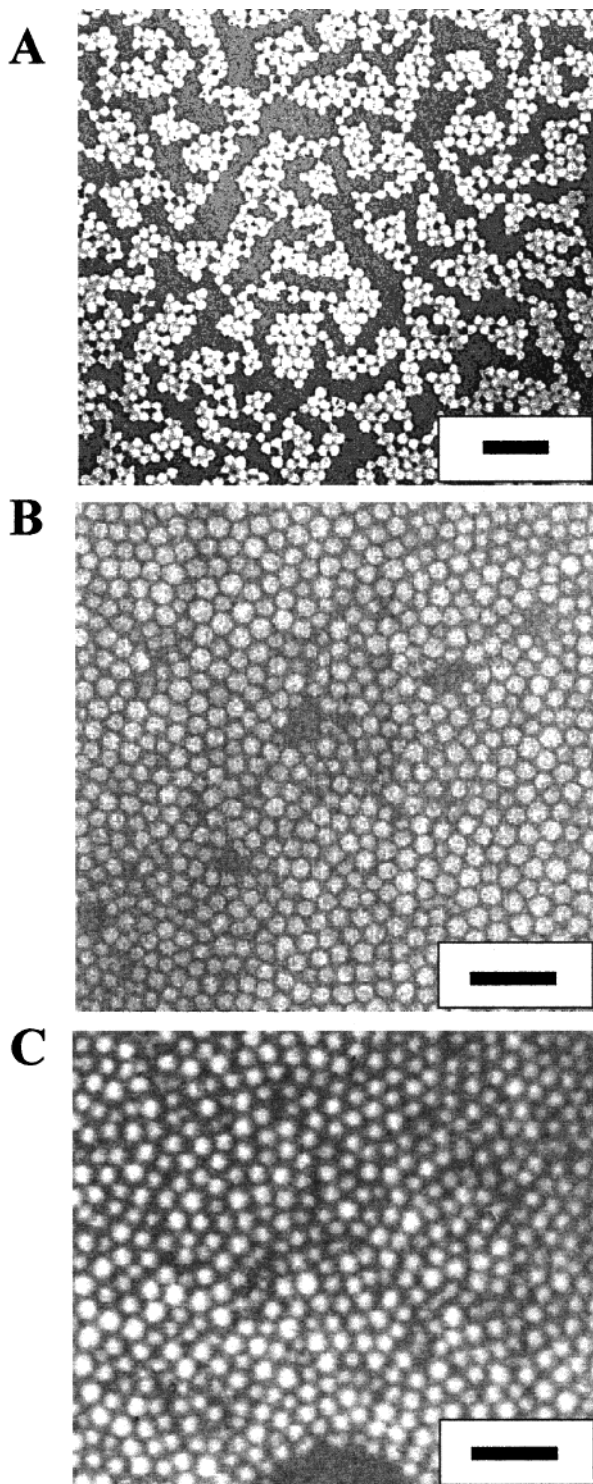


**Figure 4.** TEM pictures of microgels without a shell of polystyrene chains (A) and with a shell of polystyrene chains with  $M_w(\text{PS}) = 4200$  g/mol (B) and  $M_w(\text{PS}) = 9900$  g/mol (C). The black scale bars correspond to 100 nm.

**Table 1. Particle Characteristics Determined by Light Scattering ( $M_w(\text{Core})$ ,  $R_H(\text{Core})$ ,  $R_H(\text{Hairy Sphere})$ ) and GPC ( $M_w(\text{PS Hairs})$ ,  $M_w = \text{Molecular Weight}$ ,  $R_H = \text{Hydrodynamic Radius}$ )<sup>a</sup>**

$M_w(\text{core})$ , g/mol	$M_w(\text{PS hairs})$ , g/mol	$R_H(\text{core})$ , nm	$R_H(\text{hairy sphere})$ , nm	$\langle N_{\text{hair}} \rangle$ ( $N_{\text{GPC}}$ , $N_{\text{UV}}$ , $N_{\text{RI}}$ )
$4.0 \times 10^6$	4200	14.3	16.8	150 (70, 156, 194)
$2.3 \times 10^6$	4200	10.3	16.6	310 (290, 298, 339)
$2.3 \times 10^6$	9900	10.3	18.3	180 (190, 175, 175)
$1.7 \times 10^6$	4200	8.0	14.8	295 (300, 307, 281)
$1.7 \times 10^6$	9900	8.0	17.6	330 (320, 326, 341)
$1.7 \times 10^6$	16 800	8.0	23.1	150 (150, 139, 152)

<sup>a</sup> The average number of hairs per particle ( $\langle N_{\text{hair}} \rangle$ ) has been determined from the PS peak of the GPC elugram ( $N_{\text{GPC}}$ ) (see Figure 3), by UV/vis absorption spectroscopy ( $N_{\text{UV}}$ ), and from the refractive index of the hairy spheres (see eq 1) ( $N_{\text{RI}}$ ) measured at  $\lambda = 633$  nm.

ticles without polymer coating are in close contact also in the TEM picture (Figure 4a).

The hydrodynamic radii determined by dynamic light scattering of colloidal particles before and after grafting are given in Table 1. For the grafted particles, a distinct increase in hydrodynamic radius is found.

At a given core size, the hydrodynamic radius of the particles is increasing with molecular weight of the PS hairs. Importantly, the number of hairs per single particle in all cases is much larger than 100, corresponding to a comparatively high surface grafting density of larger than 1 chain per  $(2.5 \text{ nm})^2$ . Whereas the molecular weight of the PS hairs does not influence the grafting density up to  $M_w = 9900$  g/mol, there seems to be a slight decrease in the grafting efficiency for the longest hairs with  $M_w = 16\,800$  g/mol. This effect most probably is caused by steric constraints. Especially for macromers with high molecular weight, the reactive sites on the polyorganosiloxane surface are blocked by grafted hairs. This makes the coupling of additional macromers more difficult. Taking into account the small size of our polyorganosiloxane microgels, the grafting density which could be achieved by our grafting-onto technique still is very large. It is definitely sufficient to achieve our intention of compatibilization of the particles with polymeric chains, as will be seen in the final chapter of this article. Here, it should be mentioned that previously Roovers et al.<sup>19</sup> have been able to achieve also very high grafting densities by grafting very long polymer chains ( $M \leq 100\,000$  g/mol) onto nanosized functional dendrimers.

**Compatibility of PS-Grafted Microgels with Linear PS Chains.** The preparation of colloid–polymer mixtures by solution casting has been described above. A first criterion of compatibility was the optical transparency of these films. In case the colloidal particles are homogeneously distributed all over the polymer matrix, due to the small particle size highly transparent films should be obtained even at high particle concentrations. On the other hand, in the case of depletion demixing large colloidal clusters are formed. Because of the strong light scattering intensity of such large aggregates, these inhomogeneous samples look turbid. According to this qualitative criterion of colloid–polymer compatibility, homogeneous, i.e., transparent, mixtures have been obtained if the molecular weight of the grafted PS macromers was at least as large as the molecular weight of the matrix polymer chains.

The microscopic bulk structure of the colloid–polymer films has been studied by TEM. For this purpose, several slices with thickness a few micrometers have been cut from the composite film. Figure 5 shows a series of typical TEM images.

A sample containing only 1 wt % colloidal particles without PS-grafted surface in a matrix of PS chains ( $M_w = 4200$  g/mol) (Figure 5, I) shows the formation of large



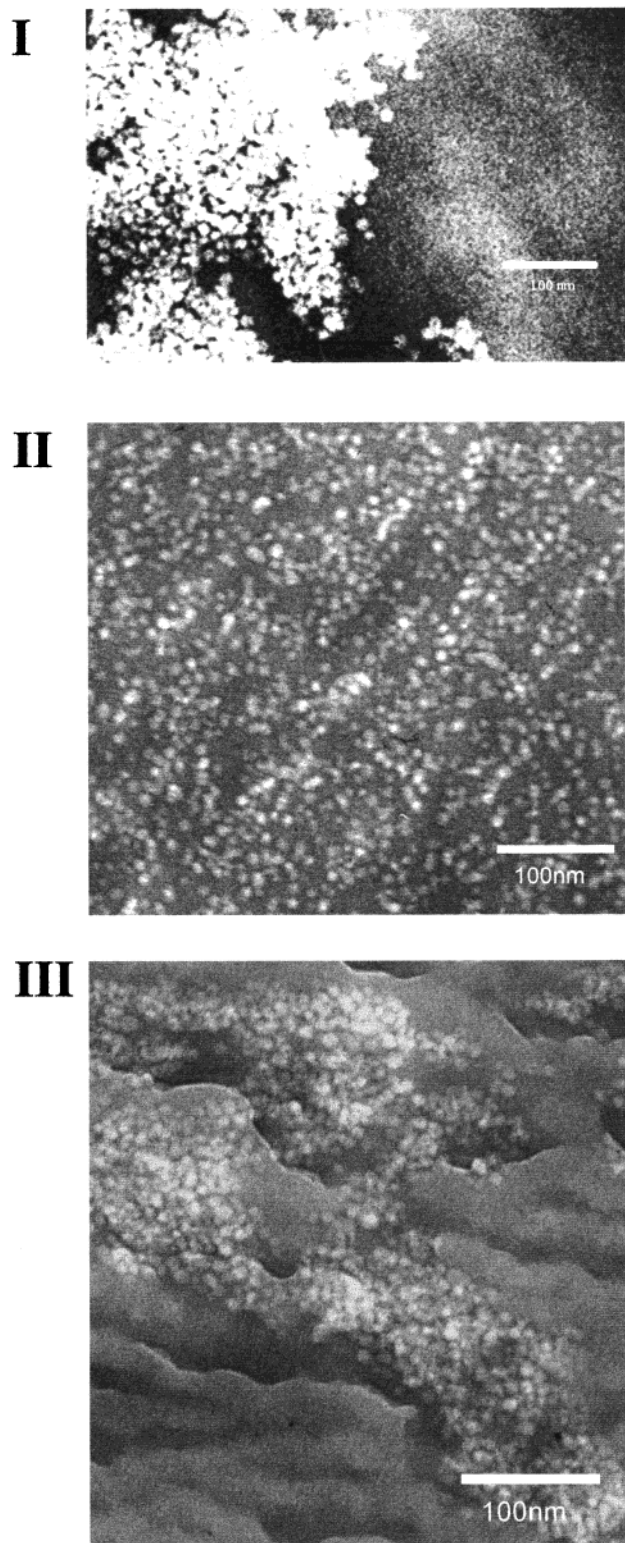


**Figure 5.** TEM pictures of polymer–colloid mixtures containing 1 wt % microgels without a shell of polystyrene chains and 99 wt % PS chains ( $M_w = 4200$  g/mol) (I), 30 wt % microgels with a shell of polystyrene chains ( $M_w = 9900$  g/mol) and 70 wt % PS chains ( $M_w = 4200$  g/mol) (II), 15 wt % microgels with a shell of polystyrene chains ( $M_w = 4200$  g/mol) and 85 wt % PS chains ( $M_w = 16\,800$  g/mol) (III). The white scale bars correspond to 100 nm.

colloidal clusters besides regions free of colloidal particles. This system, which is also optically nontransparent, is inhomogeneous in structure due to depletion demixing. On the other hand, a mixture of microgels

grafted with PS macromers ( $M_w = 9900$  g/mol) and PS chains ( $M_w = 4200$  g/mol) (Figure 5, II) even at high particle concentration shows a uniform homogeneous structure. In this case, depletion demixing seems to be suppressed. The final example, a mixture of microgels grafted with PS macromers ( $M_w = 4200$  g/mol) and PS chains ( $M_w = 16\,800$  g/mol) (Figure 5, III), looks similar in structure as Figure 5, I. Therefore, depletion demixing is also found if the matrix chains are longer than the polymacromer hairs. This is a general finding of our studies, which comprised any combination of the colloidal particles and the polymeric chains given in Table 1.

For a more detailed analysis of the structure of the colloid–polymer mixtures, small-angle X-ray scattering has been used. Here, it should be noted that there is a contrast in electron density between the microgel cores on one hand and both the grafted PS hairs and the PS chains on the other. Therefore, only the microgel cores embedded in a matrix of PS are visible in the SAXS experiment. The scattering curves (see Figure 6a,b) show a well-pronounced structure peak at small  $s$ , which provides a measure for the interparticle distance between the microgel cores. At larger  $s$ , there are weak oscillations visible corresponding to the particle form factor of the microgel cores.

The samples whose SAXS intensities are shown in Figure 6 each consisted of 45 wt % of identical spherical brushes ( $M_{w,\text{hair}} = 9900$  g/mol) in three different matrix polymers ( $M_w = 600, 4200$ , and  $16\,800$  g/mol). If the matrix molecular weight is smaller than that of the hairs, the peak position and therefore the mean distance between colloidal particles in both cases are identical, while the peak height and peak sharpness are increasing with increasing hair length (Figure 6 a,b). There is a dramatic change if grafted hairs are shorter than the matrix chains (Figure 6c). In this case, the structure peak not only is much less pronounced than in the other two cases, but its position is also shifted toward smaller  $s$ , corresponding to an increase in interparticle spacing detected by SAXS. This deviation in interparticle spacing for the last sample (Figure 6c) is interpreted as follows: the particles tend to form clusters, and as a consequence, the average spacing between particles is larger than in the case of a homogeneous particle distribution. Also, the structure peak in this case nearly disappears for this sample, signifying that the interparticle spacing in comparison to the samples with hair length larger than the chain length (Figure 6a,b) is defined only very roughly.

For a more quantitative analysis of our SAXS measurements, we have applied the paracrystalline fitting method.<sup>20</sup> This method is used to calculate trial SAXS profiles assuming a certain particle shape and interparticle arrangement. In our case, analogous to our previous SAXS results for spherical copolymer micelles in a homopolymer melt,<sup>8,9</sup> we chose spherical particles on a face-centered-cubic lattice (fcc). Fitting parameters are the edge of the cubic lattice  $a$ , the lattice distortion  $\Delta a/a$ , the particle radius  $R$  (of the microgel core!), radius polydispersity  $\Delta R/R$ , and the interface roughness. The best results of this fitting procedure for the SAXS data shown in Figure 6 are summarized in Table 2. Interestingly, the core radius of 6.5 nm is smaller than the hydrodynamic radius determined by dynamic light scattering (8 nm). Probably, the porosity of the microgels causes an increase in hydrodynamic friction.

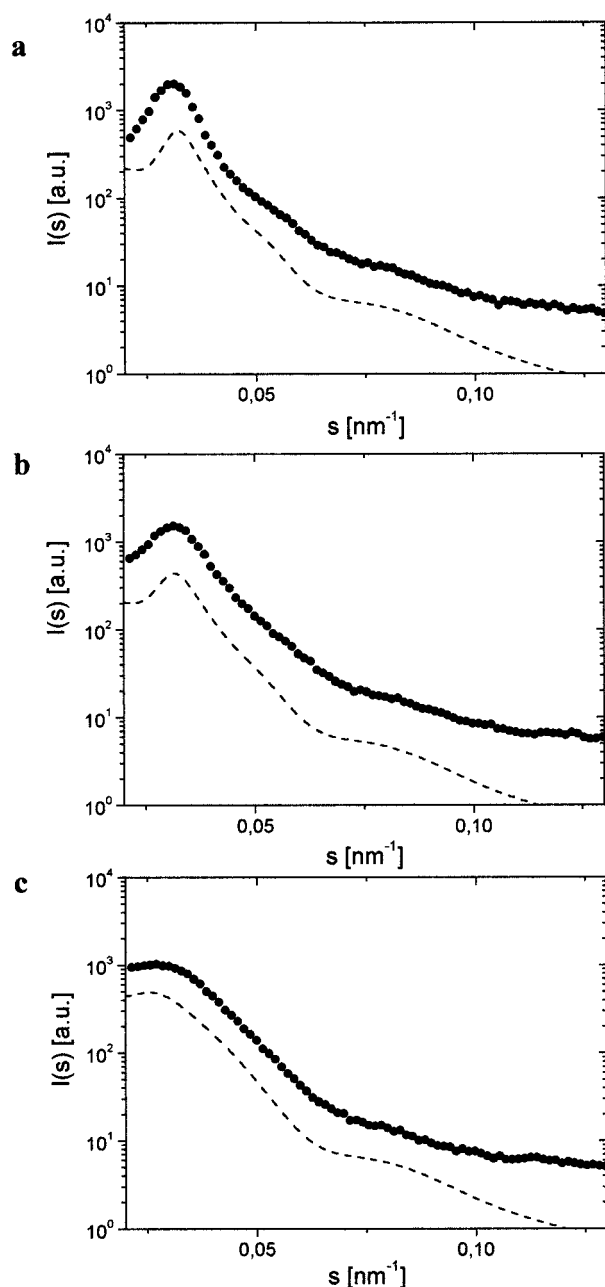


**Figure 6.** Scattered intensities measured by SAXS (symbols) for samples containing 45 wt % of hairy spheres ( $M_{w,\text{hair}} = 9900$  g/mol) in different matrix polymers (a:  $M_w = 600$  g/mol; b:  $M_w = 4200$  g/mol; c:  $M_w = 16\,800$  g/mol). Dashed lines correspond to best fits according to the paracrystalline fitting model. Fitting parameters are given in Table 2.

Therefore, opposite to compact spheres, the effective hydrodynamic radius of the microgels could be larger than their geometrical radius. This problem, however, does not effect the interpretation of the results discussed in this article. The parameters characterizing the interparticle spacing ( $a$  and  $\Delta a/a$ ) are in agreement with the qualitative discussion of the structure peak

given above, i.e., identical interparticle distances ( $a$ ) for samples a and b and a distinct increase in particle distance ( $a$ ) and structural disorder ( $\Delta a/a$ ) if the length of the PS chains exceeds that of the PS hairs (sample c).

To use the fitting results of our SAXS data as a criterion for the compatibility of grafted colloids and polymer chains, the particle volume fraction of microgel cores  $\phi_{\text{SAXS}}$  has been calculated from the fit parameters according to

$$\phi_{\text{SAXS}} = 4 \frac{\frac{4}{3}\pi R^3}{a^3} \quad (2)$$

$\phi_{\text{SAXS}}$  is compared to the volume fraction  $\phi$  determined from the sample composition, i.e., 45 wt % PS-grafted microgels, corresponding to 15 vol % microgel cores in a matrix of PS if we assume comparable densities of the colloidal particles and the PS matrix. This assumption is in agreement with previous density measurements of polyorganosiloxane microgels.<sup>14</sup> Here, it should be noted once again that only the microgel cores are detected in the SAXS experiment. Polyorganosiloxane core volume fractions as determined by SAXS and from the sample composition for the three samples shown in Figure 6 are also summarized in Table 2. For the two samples with PS hairs longer than the PS matrix chains,  $\phi_{\text{SAXS}}$  and  $\phi$  agree quite well. The minor deviation could be due to the neglect of the particle size polydispersity  $\Delta R/R$  of about 20% or neglect of the lattice distortion factor  $\Delta a/a$  in eq 2. This agreement seems to justify the assumption of a distorted fcc lattice, which proves the homogeneous distribution of the colloidal particles within the PS matrix. On the other hand, the last sample (Figure 6 c) shows a strong deviation of  $\phi_{\text{SAXS}}$  from  $\phi$ . Therefore, the assumption of a homogeneous particle distribution is found to be wrong for mixtures containing hairy spheres in a matrix of linear chains in case the chains are longer than the hairs.

**Qualitative Model for Compatibility of Hairy Spheres and Linear Chains.** Finally, let us try to explain our experimental findings. To understand the influence of the molecular weight of the grafted polymer hairs with respect to the molecular weight of the matrix chains on colloid–polymer compatibility, we have developed the semiquantitative model sketched in Figure 7.

Most important, in contrast to ordinary colloidal particles, our hairy spheres have no rigid noninterpenetrable surface. Therefore, if two hairy spheres come into close contact, their polymer coatings may partially interpenetrate. Therefore, their effective particle radius should be in between their core radius and their total radius, as sketched by the dotted circles in Figure 7. Not only the colloidal particles can interpenetrate each other, but also the matrix chains can partially penetrate into the polymer shell of the hairy sphere. The smaller

**Table 2.** Fitting Parameters for Paracrystalline Fits Shown in Figure 6 (Core Size  $R$ , Size Polydispersity  $\Delta R/R$ , Length of fcc Cell  $a$ , and Lattice Distortion  $\Delta a/a$ ), and Volume Fraction  $\phi_{\text{SAXS}}$  Calculated from These Parameters (See Eq 2) in Comparison to the Volume Fraction  $\phi$  Determined from the Sample Composition

sample (45 wt % grafted spheres with $M_{\text{hair}} = 9900$ )	$R$ [nm]	$\Delta R$ [nm]	$a$ [nm]	$\Delta a/a$	$\phi_{\text{SAXS}}$	$\phi$
$M_{\text{chain}} = 600$ (a)	6.4	1.2	32.5	0.22	0.13	0.15
$M_{\text{chain}} = 4200$ (b)	6.4	1.2	32.5	0.25	0.13	0.15
$M_{\text{chain}} = 16800$ (c)	6.4	1.2	34.0	0.40	0.11	0.15



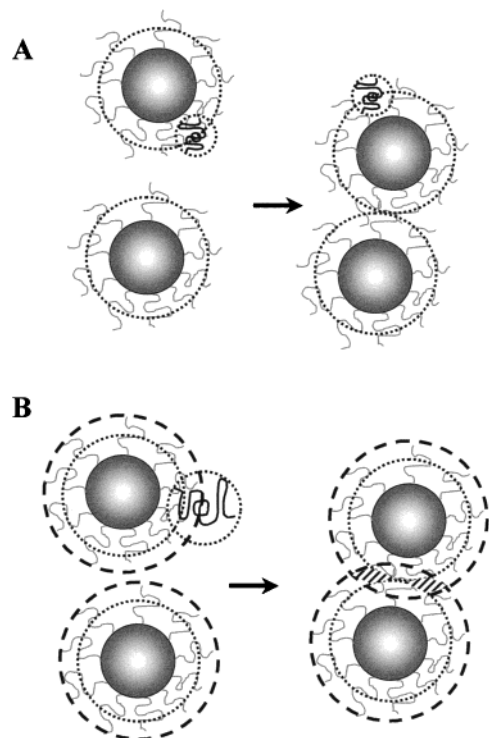


**Figure 7.** Sketch of the suppression of depletion demixing (see Figure 1) for colloidal particles with a shell of polymer chains ("hairs" → "hairy spheres"), embedded in a matrix of linear polymer chains. If the linear chains are shorter than the "hairs", depletion is completely suppressed (A). If the linear chains are longer than the "hairs", the system practically resembles the standard mixture of colloidal particles and linear chains (see Figure 1), and depletion demixing of hairy spheres and linear chains is found (B).

the matrix chain, the further it may enter the polymer corona. This leads us to two possible scenarios:

(A) In case the center of mass of the polymeric chain, i.e., the center of the dotted circles drawn around the polymer coils in Figure 7, may approach the colloidal core of a hairy sphere beyond its effective particle radius, there is no gain in free volume (and in entropy) for the polymer chain upon aggregation of the colloidal particles (Figure 7A). Therefore, there would be only an entropy loss due to aggregation of the spherical colloids, and entropy in this case favors a homogeneous particle configuration. As a consequence, colloid–polymer mixtures containing hairy spheres with hair length equal or longer than the matrix chains do not show depletion demixing.

(B) In case the matrix chains are longer than the polymer hairs, the center of mass of these chains may not penetrate into the polymer corona up to the effective particle size. In this case, like in the case of colloidal particles with rigid nonpenetrable surfaces and polymer coils (see Figure 1), an excluded volume zone is found around the hairy spheres (dashed circle, Figure 7B). If two hairy spheres come into close contact, their excluded-volume zones overlap, thereby reducing the total excluded volume and increasing the free volume of the polymer chains. This scenario sketched in Figure 7B is practically identical to the scenario sketched in Figure 1, and such systems of hairy particles embedded in a high molecular weight matrix therefore are expected to exhibit depletion demixing.

In summary, the compatibility of polymer chains and colloidal particles may be largely enhanced by polymer

coating of the later in case the molecular weight of the polymer hairs is at least as large as that of the polymer matrix chains.

## Conclusions

In this article, we have presented a method to prepare nanosized spherical colloids grafted with PS chains. The grafting density, i.e., the number of hairs per particle in respect to the particle size, was comparatively large even for longer polymer hairs of molecular weight about 17 000 g/mol. Using our new colloids, we have been able to prepare optically transparent colloid–polymer mixtures with homogeneous microscopic structure. Importantly, we found that the molecular weight of the polymer hairs in respect to the molecular weight of the matrix polymers plays a very important role for compatibilization. This effect has been explained semiquantitatively by an enhanced depletion model, taking into account the probability of interpenetration of the hairy sphere particle surface.

In a subsequent publication, we are going to discuss how concentration and topology of the colloidal particles, i.e., the hair length with respect to the length of the matrix chains, effect the mechanical properties of the homogeneous composite materials.

**Acknowledgment.** The authors thank Wacker Corp., Burghausen, Germany, for providing the silane monomers and the Pt catalyst used for the grafting reaction. Rudolf Würfel is thanked for taking the TEM pictures of the colloidal particles and of the colloid–polymer mixtures shown in this article. This work was financially supported by the Deutsche Forschungsgemeinschaft, Grant SFB 262, Project D23, and by the Materialwissenschaftliches Forschungszentrum of the University of Mainz.

## Appendix

**Preparation of Polyorganosiloxane Microgels with Si–H Surface Groups.** In a 2 L three-necked, round-bottomed flask equipped with a mechanical stirrer, 30 g of an aqueous solution containing 10 wt % of the surfactant dodecylbenzenesulfonic acid is mixed with 1470 g of distilled water (Milli-Q). Upon stirring, during 3 h 300 g of the monomer trimethoxymethylsilane is added dropwise at room temperature. This mixture is stirred for another 6 h and then filtered, yielding a transparent slightly opaque dispersion. Upon stirring, 60 g of the end-capping agent tetramethyldisiloxane is added dropwise to 1000 g of this dispersion. After stirring overnight the dispersion is destabilized by dropping it into 2 L of saturated NaCl solution (20 wt %). The white precipitate is filtered off and washed thoroughly with Milli-Q water and, finally, washed once with methanol. The wet precipitate is redispersed in 800 mL of toluene, dried over sodium sulfate, and filtered. The remaining water and methanol are evaporated, and the end-capping and surface-functionalization reaction is completed by adding once more tetramethyldisiloxane (18 g per 500 g of toluene solution). After stirring overnight, the solvent is evaporated at 40 °C and 64 mbar vacuum, and the SiH end-capped microgels are freeze-dried in benzene.

## References and Notes

- (1) Asakura, S.; Oosawa, F. *J. Chem. Phys.* **1954**, *22*, 1255.
- (2) Vrij, A. *Pure Appl. Chem.* **1976**, *48*, 471.

- (3) Poon, W. C. K.; Pusey, P. N. In *Observation, Prediction and Simulation of Phase Transitions in Complex Fluids*; Baus, M., et al., Eds.; Kluwer Academic Publishers: Norwell, MA, 1995; pp 3–51.
- (4) Bechinger, C.; Rudhardt, D.; Leiderer, P.; Roth, R.; Dietrich, S. *Phys. Rev. Lett.* **1999**, *83*, 3960.
- (5) Yuan, Q. W.; Mark, J. E. *Macromol. Chem. Phys.* **1999**, *200*, 206.
- (6) McCarthy, D. W.; Mark, J. E. *Rubber Chem. Technol.* **1998**, *71*, 941.
- (7) Schärfl, W.; Tsutsumi, K.; Kimishima, K.; Hashimoto, T. *Macromolecules* **1996**, *29*, 5297.
- (8) Schärfl, W. *Macromol. Chem. Phys.* **1999**, *200*, 481.
- (9) Gohr, K.; Pakula, T.; Tsutsumi, K.; Schärfl, W. *Macromolecules* **1999**, *32*, 7156.
- (10) Gohr, K.; Schärfl, W. *Macromolecules* **2000**, *33*, 2129.
- (11) Baumann, F.; Schmidt, M.; Deubzer, B.; Geck, M.; Dauth, J. *Macromolecules* **1994**, *27*, 6102.
- (12) Baumann, F.; Deubzer, B.; Geck, M.; Dauth, J.; Schmidt, M. *Macromolecules* **1997**, *30*, 7568.
- (13) Graf, C.; Schärfl, W.; Fischer, K.; Hugenberg, N.; Schmidt, M. *Langmuir* **1999**, *15*, 6170.
- (14) Graf, C.; Schärfl, W.; Maskos, M.; Schmidt, M. *J. Chem. Phys.* **2000**, *112*, 3031.
- (15) Roos, C.; Schmidt, M.; Ebenhoch, J.; Baumann, F.; Deubzer, B.; Weis, J. *Adv. Mater.* **1999**, *11*, 761.
- (16) Schärfl, W.; Roos, C. *Phys. Rev. E* **1999**, *60*, 2020.
- (17) Schärfl, W.; Lindenblatt, G.; Strack, A.; Dziezok, P.; Schmidt, M. *Prog. Colloid Polym. Sci.* **1832**, *110*, 285.
- (18) Marciniak, B.; Gulinski, J. In *Comprehensive Handbook of Hydrosilylation*; Urbaniak, W., Kornetka, Z. W., Eds.; Pergamon Press: Oxford, 1992.
- (19) Roovers, J.; Zhou, L. L.; Toporowski, P. M.; van der Zwan, M.; Iatrou, H.; Hadjichristidis, N. *Macromolecules* **1993**, *26*, 4324.
- (20) Matsuoka, H.; Tanaka, H.; Hashimoto, T.; Ise, N. *Phys. Rev. B* **1987**, *36*, 1754.

MA001328F